



ELSEVIER

Thermochimica Acta 266 (1995) 119–127

thermochimica  
acta

## Relationship between enthalpy relaxation and dynamic mechanical relaxation of engineering plastics<sup>☆</sup>

Hirohisa Yoshida

*Department of Industrial Chemistry, Tokyo Metropolitan University, Minami-Osawa, Hachioji,  
Tokyo 192-03, Japan*

---

### Abstract

The enthalpy relaxation and dynamic modulus relaxation processes of amorphous poly(ether imide) (PEI) and two types of crystalline poly(aryl-ether-ether-ketone) (PEEK), low and high crystallinity, were analyzed by the Kohlrausch–Williams–Watts equation. Both crystalline PEEKs and amorphous PEI showed almost the same relationship between enthalpy relaxation time and  $T_g - T_a$  in the temperature difference range  $10 \text{ K} < T_g - T_a < 25 \text{ K}$ . The enthalpy relaxation time was increased slightly with the increase in degree of crystallinity at a given  $T_g - T_a$ . A good correlation was observed between the enthalpy relaxation time and the dynamic modulus relaxation time for both PEI and PEEK, in particular, a linear relationship with slope equal to unity was obtained for PEI.

*Keywords:* Dynamic mechanical relaxation; Enthalpy relaxation; Physical ag Poly(aryl-ether-ether-ketone); Poly(ether imide)

---

### 1. Introduction

When the glassy state, essentially the thermodynamic non-equilibrium state, is held at temperatures near the glass transition temperature ( $T_g$ ), excess thermodynamic quantities relax toward the thermodynamic equilibrium state. As the rate of relaxation accelerates with increasing temperature, the relaxation phenomenon is clearly recognized in the temperature region close to  $T_g$ . These phenomena are known as enthalpy relaxation and/or volume relaxation according to the observed thermodynamic quantity. These phenomena have been reported for inorganic, organic and polymeric

---

<sup>☆</sup> Dedicated to Hiroshi Suga on the Occasion of his 65th Birthday.

materials [1–3]. Suga and coworkers [2, 4–8] reported the quantitative analysis of the enthalpy relaxation process for the glassy state and the glassy crystal state of various pure materials measured by adiabatic calorimetry.

We have reported the numerical analysis of enthalpy relaxation using excess enthalpy observed by differential scanning calorimeter to investigate the effects of primary and secondary structures on the rate of enthalpy relaxation of polymeric materials [9–13]. According to the effects of the chemical structure [9] and hydrogen bonding formation [10] on the rate of enthalpy relaxation, the enthalpy relaxation of polymers occurs as a result of internal rotation of the main chain toward reducing configurational energy. At a given normalized annealing temperature ( $T_g - T_a$ ), the rate of enthalpy relaxation of engineering plastics is faster than that of conventional glassy polymers, although  $T_g$  values of engineering plastics are higher than those of glassy polymers [14, 15]. We have also pointed out that engineering plastics are characterized by superior toughness in spite of their glassy nature because of the release of inner stress through internal rotation of the main chains [14, 25].

Following a similar annealing with enthalpy relaxation, mechanical properties such as stress relaxation [16] and creep relaxation behaviors [17], diffusion properties [18], mechanical strength [19] and dynamic viscoelastic properties [20, 21] of polymers are influenced. These phenomena are known as physical aging [17]. However, the relation between enthalpy relaxation and physical aging has not been clarified. In this study, the correlation between thermodynamic relaxation and physical aging was estimated by comparing the rate of enthalpy relaxation and dynamic modulus relaxation for amorphous and crystalline engineering plastics.

## 2. Experimental

### 2.1. Sample

Poly(aryl-ether-ether-ketone) (PEEK) (ICI Co. Ltd., 450G) and poly(ether imide) (PEI)(GE Co. Ltd., Ultem) were used in the experiments. Two types of PEEK film were prepared by the following methods. Quenched PEEK was obtained by fast-cooling (more than  $300 \text{ K s}^{-1}$ ) from 658 to 273 K. The slow-cooled PEEK was obtained by cooling at  $20 \text{ K min}^{-1}$  from 658 K to room temperature. PEI quenched film was obtained by quenching from 553 K into water at 273 K. The preliminary X-ray analysis of PEI and the quenched PEEK showed a typical amorphous halo. Samples were annealed at various temperatures below  $T_g$  in the instruments.

### 2.2. Differential scanning calorimetry (DSC)

The thermal properties of the samples were measured using a Seiko DSC 200, connected with a Seiko thermal analysis system SSC5200, at  $10 \text{ K min}^{-1}$  under dry nitrogen gas flow. The glass transition temperature ( $T_g$ ) and heat capacity ( $C_p$ ) were measured at  $10 \text{ K min}^{-1}$  as reported previously [22, 23].

Each sample was heated to 10 K above its  $T_g$  in order to eliminate thermal history, and then quenched to the annealing temperature at  $40 \text{ K min}^{-1}$  where it was held for a fixed period in the DSC. After annealing, the  $C_p$  of the annealed sample ( $C_{p\text{anneal}}$ ) was measured in the temperature range from  $T_a - 20$  to  $T_g + 20$  K (except the quenched PEEK which was heated from  $T_a - 20$  to  $T_g + 15$  K to eliminate cold-crystallization during  $C_p$  measurement) at  $10 \text{ K min}^{-1}$ . The  $C_p$  of the unannealed sample ( $C_{p\text{unanneal}}$ ), which was quenched to the starting temperature of  $C_p$  measurement after  $C_p$  measurement of the annealed sample, was also measured in the same temperature range as the  $C_p$  of the annealed sample. The reduced enthalpy ( $\Delta H$ ) during annealing was obtained by the equation [9]

$$\Delta H = \int_{T_1}^{T_2} C_{p\text{anneal}} dT - \int_{T_1}^{T_2} C_{p\text{unanneal}} dT \quad (1)$$

### 2.3. Dynamic mechanical analysis (DMA)

The dynamic viscoelastic properties of the samples were measured by a Seiko DMA 100 connected with a Seiko thermal analysis system SSC5200. Before measuring the dynamic viscoelastic properties, PEI and the slow-cooled PEEK were quenched once from  $T_g + 20$  K (the quenched PEEK was quenched from  $T_g + 15$  K) and the samples placed in the DMA instrument which was held at the annealing temperature. The dynamic viscoelastic properties of samples were measured isothermally as a function of annealing time in the frequency range from 0.02 to 50 Hz.

## 3. Results and discussion

The DSC heating curves of the quenched PEEK showed a glass transition at 420 K, a sharp exothermic peak due to cold-crystallization at 450 K, and a broad melting endothermic peak at 610 K. Instead of a sharp exothermic cold-crystallization peak, the DSC heating curve of the slow-cooled PEEK showed a broad, small pre-melt crystallization peak from 530 to 580 K. The degrees of crystallinity of the two PEEKs were evaluated by their heats of fusion. For calculations of the degree of crystallinity,  $130 \text{ J g}^{-1}$  heat of fusion was assumed for the perfect crystal phase of PEEK [24]. By considering the heat of cold-crystallization, the degree of crystallinity of the quenched and slow-cooled PEEKs were 0.04 and 0.22, respectively. The  $T_g$  of the quenched and slow-cooled PEEKs were 417.2 and 418.3 K, respectively. The heat capacity difference between the glassy state and the liquid state at  $T_g$  ( $\Delta C_p$ ), which was calibrated by the degree of crystallinity, was  $0.270 \text{ J K}^{-1} \text{ g}^{-1}$  for the quenched PEEK and  $0.173 \text{ J K}^{-1} \text{ g}^{-1}$  for the slow-cooled PEEK. In the case of crystalline polymers, amorphous chains between crystal lamellae are extended on crystallization, because the amorphous chains are trapped in the crystal lamellae. Under such conditions, the conformation of the amorphous chains may become ordered with crystallization. In this study, a two-phase model (amorphous and crystalline regions) was used to evaluate the degree

of crystallinity. A three-phase model considering the intermediate region was proposed to apply the structure of the crystalline polymer [28]. The difference in  $\Delta C_p$  between the quenched and slow-cooled PEEKs was probably caused by conformational difference that appeared on crystallization and by the method of estimating the crystallinity.

The changes in reduced enthalpy ( $\Delta H$ ) caused by annealing at temperatures below  $T_g$  are shown in Fig. 1 for the quenched PEEK (a) and the slow-cooled PEEK (b). The changes in  $\Delta H$  for the slow-cooled PEEK were smaller than those for the quenched PEEK at a given temperature, because of the high crystallinity of the slow-cooled PEEK. The changes of  $\Delta H$  in PEI are shown in Fig. 2; the data were analyzed and reported previously [14]. The changes in the frequency dependency of the dynamic modulus ( $E'$ ) for PEI observed as a function of annealing time at 466 K are shown in Fig. 3. With annealing,  $E'$  increased and the frequency dependency became small. Fig. 4 shows changes in  $E'$  observed at 1 Hz at various annealing temperatures for the quenched PEEK (a) and PEI (b).

The non-exponential and non-linear relaxation process is described well by the Kohlrausch–Williams–Watts (KWW) [26] stretched exponential function  $\phi(t_a)$  given by

$$\phi(t_a) = \exp[-(t/\tau)^\beta] \quad (2)$$

where  $\tau$  and  $\beta$  are the relaxation time and a parameter corresponding to the relaxation time distribution, respectively. The adiabatic calorimetric results of enthalpy relaxation in KCN–KBr mixed crystals have been analyzed successively by the KWW equation [5]. The experimental data of the enthalpy relaxation in poly(vinyl methyl ether) are described adequately by the following KWW equation [27]

$$\Delta H(t_a, T_a) = \Delta H_\infty(T_a)[1 - \phi(t_a)] \quad (3)$$

where  $\Delta H(t_a, T_a)$  and  $\Delta H_\infty(T_a)$  indicate reduced enthalpies at annealing times  $t_a$  and  $t_\infty$  at  $T_a$ , respectively. The dynamic modulus relaxation process was also analyzed using

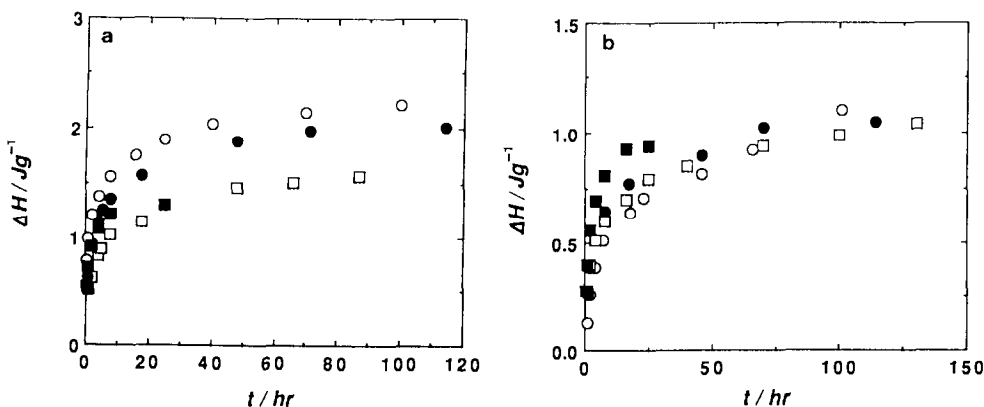


Fig. 1. Changes in reduced enthalpy ( $\Delta H$ ) at 398 (○), 403 (●), 408 (□) and 413 (■) K in the quenched PEEK (a) and slow-cooled PEEK (b).

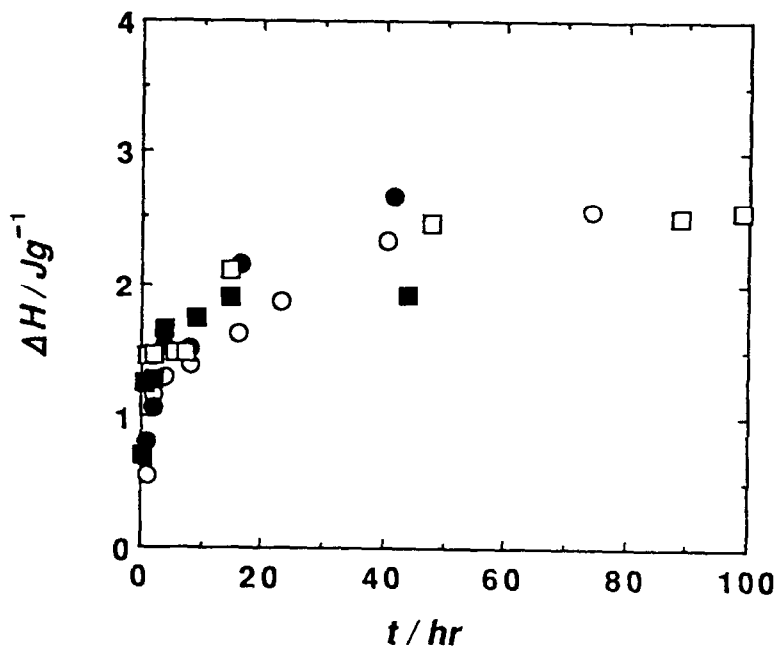


Fig. 2. Changes in reduced enthalpy ( $\Delta H$ ) at 463 (○), 466 (●), 469 (□) and 472 (■) K in PEI.

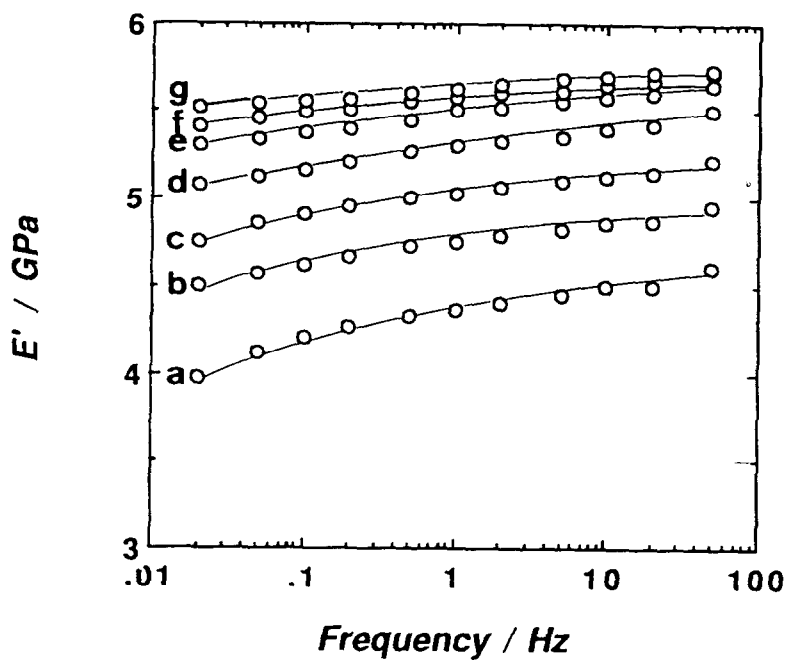


Fig. 3. Changes in frequency dependency of the dynamic modulus ( $E'$ ) for PEI at 0 (a), 0.5 (b), 1 (c), 2 (d), 4 (e), 8 (f) and 24 (g) h at 466 K.

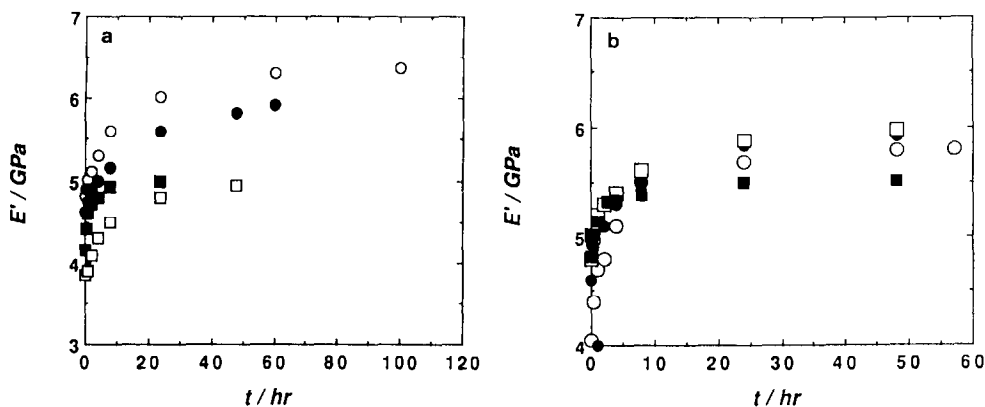


Fig. 4. Changes in dynamic modulus ( $E'$ ) measured at 1 Hz at 398 (○), 403 (●), 408 (□) and 413 (■) K for quenched PEEK (a) and at 463 (○), 466 (●), 469 (□) and 472 (■) K for PEI (b).

Eq. (2) as follows

$$\Delta E'(t_a, T_a) = E'(t_a, T_a) - E'_0(T_a) = \Delta E'_\infty(T_a) [1 - \phi](t_a) \quad (4)$$

$$\Delta E'_\infty(T_a) = E'_\infty(T_a) - E'_0(T_a) \quad (5)$$

where  $E'_0(T_a)$ ,  $E'(t_a, T_a)$  and  $E'_\infty(T_a)$  indicate  $E'$  values for the unannealed sample, the relaxed sample annealed for  $t_a$ , and the infinitely annealed sample at  $T_a$ , respectively.

The enthalpy relaxation process was analyzed by Eq. (3) using a non-linear least-squares fit of the experimental data shown in Figs. 1 and 2. The obtained values of enthalpy relaxation time ( $\tau_H$ ),  $\beta_H$  and  $\Delta H_\infty(T_a)$  are shown in Table 1 (PEI), Table 2 (quenched PEEK) and Table 3 (slow-cooled PEEK). The dynamic modulus relaxation process was also analyzed by Eq. (4). The parameters obtained by a non-linear least-squares fit of data shown in Fig. 4 are also listed in Table 1 (PEI), Table 2 (quenched PEEK) and Table 3 (slow-cooled PEEK). The standard deviations of non-linear fitting in enthalpy relaxation and dynamic modulus relaxation were about 0.1. Although the parameter  $\beta$  showed a large scattering, the value was almost constant within experimental error in this study.

Table 1

Parameters obtained by non-linear fitting of enthalpy and dynamic modulus relaxation processes for PEI

$T_a$	$\tau_H$	$\beta_H$	$\Delta H_\infty(T_a)$	$\tau_E$	$\beta_E$	$\Delta E'_\infty(T_a)$
463	1.02	0.30	5.92	1.07	0.39	1.44
466	0.68	0.43	6.10	0.79	0.36	1.23
469	0.38	0.52	6.03	0.37	0.30	1.20
472	0.29	0.45	5.67	0.21	0.37	1.17

Table 2

Parameters obtained by non-linear fitting of enthalpy and dynamic modulus relaxation processes for quenched PEEK

$T_a$	$\tau_H$	$\beta_H$	$\Delta H_x(T_a)$	$\tau_E$	$\beta_E$	$\Delta E'_x(T_a)$
398	0.52	0.60	6.69	0.67	0.55	2.42
403	0.40	0.53	6.54	0.60	0.62	2.27
408	0.29	0.53	5.33	0.59	0.54	1.83
413	0.19	0.62	5.15	0.55	0.46	1.49

Table 3

Parameters obtained by non-linear fitting of enthalpy and dynamic modulus relaxation processes for slow-cooled PEEK

$T_a$	$\tau_H$	$\beta_H$	$\Delta H_x(T_a)$	$\tau_E$	$\beta_E$	$\Delta E'_x(T_a)$
398	0.75	0.54	8.22	0.60	0.62	2.80
403	0.54	0.38	8.18	0.59	0.62	2.94
408	0.36	0.45	7.91	0.67	0.67	2.86
413	0.35	0.50	7.65	0.55	0.64	2.23

In order to compare the enthalpy relaxation rate among different polymers,  $\tau_H$  values were plotted against  $T_g - T_a$  in Fig. 5. Because the DSC method used to determine  $\Delta H$  was a dynamic method, the  $\Delta H$  observed at temperatures close to  $T_g$  contained some errors. When the PEEK data at the highest temperatures were eliminated, a linear relationship was observed between  $\log(\tau_H)$  and  $T_g - T_a$ , including PEI and both PEEKs. The estimated  $\tau_H$  value at  $T_g$  obtained by extrapolating the relationship between  $\log(\tau_H)$  and  $T_g - T_a$  to zero is about 0.08 h which agrees with the relaxation time of the glass transition evaluated by dielectric relaxation measurement for several polymers [29]. Comparing  $\tau_H$  values of PEEKs with different crystallinity in Fig. 5, the  $\tau_H$  value of the slow-cooled PEEK was slightly larger than that of the quenched PEEK. The  $T_g$  of the slow cooled PEEK was slightly higher than that of the quenched PEEK. These facts suggest the retardation effect of crystallites on the enthalpy relaxation process. For crystalline polymers, the molecular motion of internal free rotation was restricted even in the amorphous state or in the low crystallinity state. In the amorphous state of crystalline polymers, molecular conformations with low randomness may be present and internal rotation of the main chain may be difficult.

The relationship between enthalpy relaxation time ( $\tau_H$ ) and dynamic modulus relaxation time ( $\tau_E$ ) is shown in Fig. 6. Linear relationships were observed for both PEI and PEEKs. In particular, the linear relation between  $\tau_H$  and  $\tau_E$  with slope equal to unity for PEI passed through the original point; the enthalpy relaxation process was well correlated to the dynamic modulus relaxation process in amorphous polymers. This result suggested that the increase in stable conformation produced by the internal rotation of the main chain contributed to the increase in the dynamic modulus for PEI.

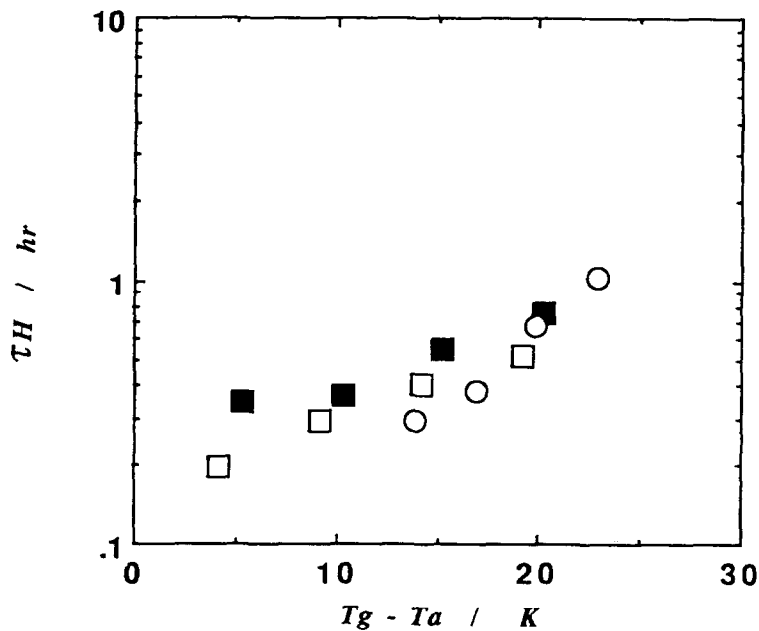


Fig. 5. Relationship between logarithmic enthalpy relaxation time ( $\tau_H$ ) and  $T_g - T_a$  for PEI (○), quenched PEEK (□) and slow-cooled PEEK (■).

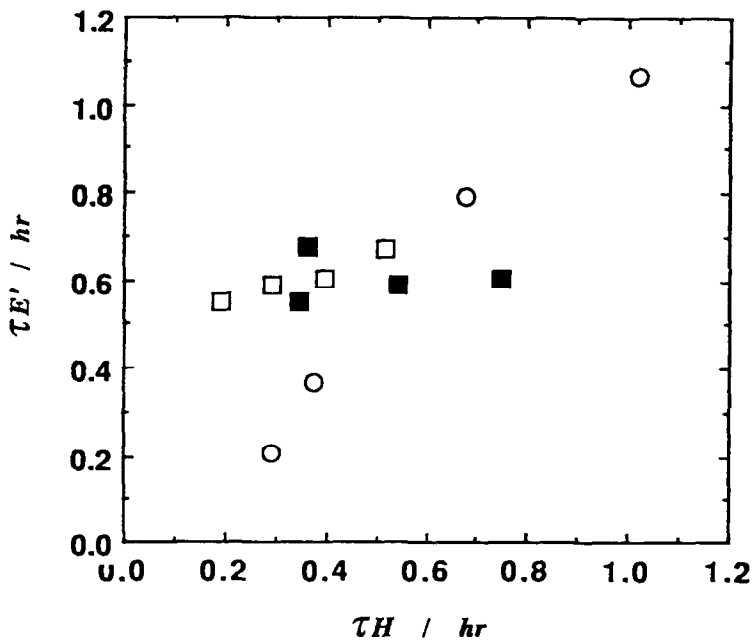


Fig. 6. Relationship between enthalpy relaxation time ( $\tau_H$ ) and dynamic modulus relaxation time ( $\tau_{E'}$ ) for PEI (○), quenched PEEK (□) and slow-cooled PEEK (■).



Although the relationship between  $\tau_H$  and  $\tau_E$  for PEEKs showed good correlations,  $\tau_E$  slightly increased with increasing  $\tau_H$ . In addition to the reason described above, the crystalline phase contributed to the dynamic modulus much more than the amorphous region for crystalline polymers.

## References

- [1] M. Goldstein and M. Nakoneczny, *Phys. Chem. Glasses*, 6 (1965) 171.
- [2] H. Suga and S. Seki, *J. Non-Cryst. Solids*, 16 (1974) 171.
- [3] A.J. Kovacs, *Forsch. Hochpolymer Forsch.*, 3 (1963) 394.
- [4] O. Haida, H. Suga and S. Seki, *Bull. Chem. Soc. Jpn.*, 50 (1977) 802.
- [5] T. Mastuo, I. Kishimoto, H. Suga and F. Luty, *Solid State Commun.*, 58 (1986) 177.
- [6] M. Oguni, H. Hikawa and H. Suga, *Thermochim. Acta.*, 158 (1990) 143.
- [7] K. Takeda, O. Yamamuro and H. Suga, *J. Phys. Chem. Solids*, 52 (1991) 607.
- [8] H. Suga, in K. Kawasaki (Ed.), *Slow Dynamics in Condensed Matter*, American Inst. Phys., New York, 1992, p. 20.
- [9] H. Yoshida and Y. Kobayashi, *J. Macromol. Sci.*, B21 (1982) 565.
- [10] H. Yoshida, K. Nakamura and Y. Kobayashi, *Polym. J.*, 14 (1982) 855.
- [11] H. Yoshida and Y. Kobayashi, *Sen-i Gakkaishi*, 37 (1981) T-458.
- [12] H. Yoshida and Y. Kobayashi, *Polym. J.*, 14 (1982) 925.
- [13] H. Yoshida and Y. Kobayashi, *Polym. Eng. Sci.*, 12 (1983) 907.
- [14] H. Yoshida, *Netsu Sokutei*, 15 (1988) 65.
- [15] K. Ejiri, M. Yamamoto and T. Hatakeyama, *Sen-i Gakkaishi*, 45 (1989) 55.
- [16] S. Matsuoka, H.E. Bair, S.S. Bearder, H.E. Kern and J.T. Ryan, *Polym. Eng. Sci.*, 18 (1978) 1073.
- [17] L.C.E. Struik, *Physical Aging in Amorphous Polymers and Other Materials*, Elsevier, Amsterdam, 1978, p. 98
- [18] H. Yoshida, R. Yoshida and Y. Kobayashi, *Sen-i Gakkaishi*, 38 (1982) T-457.
- [19] H. Yoshida and Y. Kobayashi, *Polym. Commun.*, 24 (1983) 336.
- [20] C.Y.-C. Lee and I.J. Golgarb, *Polym. Eng. Sci.*, 21 (1981) 951.
- [21] L.C.E. Struik, *Polymer*, 28 (1987) 57.
- [22] T. Hatakeyama, H. Kanetsuna and S. Ichihara, *Thermochim. Acta.*, 146 (1989) 311.
- [23] S. Nakamura, M. Todoki, K. Nakamura and H. Kanetsuna, *Thermochim. Acta*, 136 (1988) 163.
- [24] D.J. Blundell and B.N. Osborn, *Polymer*, 24 (1983) 1183.
- [25] H. Yoshida, *Netsu Sokutei*, 13 (1986) 131.
- [26] G. Williams and D.C. Watts, *Trans. Faraday Soc.*, 66 (1970) 80.
- [27] J.M. Cowie and R. Ferguson, *Polym. Commun.*, 27 (1986) 258.
- [28] S.Z.D. Cheng, Z. Wu and B. Wunderlich, *Macromolecules*, 20 (1987) 2802.
- [29] S. Saito, *Kolloid-Z.*, 189 (1963) 116.